ADVANCED MATERIALS

DOI: 10.1002/adma.200702781

Aerogel Templated ZnO Dye-Sensitized Solar Cells**

By *Thomas W. Hamann, Alex B. F. Martinson, Jeffrey W. Elam, Michael J. Pellin,* and *Joseph T. Hupp**

Dye-sensitized solar cells (DSSCs) based on nanocrystalline TiO_2 have exhibited solar energy-conversion efficiencies of over 10% and remain one of the most promising candidates for cost-effective solar energy conversion devices.[1,2] The most efficient DSSCs reported to date utilize a high surface area photoanode, which allows for good light harvesting with a moderate extinction dye, in contact with the I_3^-/I^- couple which acts as a redox mediator.[3] The good performance of DSSCs is partially attributed to the slow dark reaction, i.e., electron transfer from TiO_2 to I_3^- via a potentially multi-electron process. The slow dark reaction kinetics allows for excellent charge collection despite the relatively slow (millisecond) transport through the nanoparticle network.[4] The I_3^-/I^- couple, however, has several disadvantages, including limitations on the open-circuit voltage related to the redox potential of the mediator species.

In order to push device performance beyond its current limits, a faster redox shuttle, which requires a smaller overpotential to reduce the oxidized dye, is likely necessary, either to increase the photovoltage (provided that the dark current in not enhanced) or to allow alternate dyes with increased spectral coverage to be used. Replacing iodide/triiodide with faster one-electron, outer-sphere redox reagents such as ferrocene, however, has resulted in significantly worse overall performance.[5,6] Although such fast redox species efficiently reduce the oxidized dye, rapid recombination between electrons in the TiO_2 and the redox shuttle results in poor electron collection.[5–7] Therefore, an alternate redox shuttle will concomitantly require faster charge transport through the metal oxide frameworks to allow for complete charge collection under cell operating conditions.

Several interesting photoanode architectures have been fabricated with reduced dimensionality, a design feature that is expected to accelerate charge transport. Among these new architectures are hydrothermally grown ZnO nanorod arrays, ZnO nanotubes, and TiO_2 nanotubes.[8–10] The ZnO nanorod arrays have been shown to exhibit much faster transport than comparable ZnO nanoparticle networks.[11,12] While nanorod devices showed promising efficiencies of 1.5%, further improvement requires overcoming the technical challenge of increasing the relatively low surface area that currently limits light-harvesting.[8] Nominally one-dimensional ZnO nanotubes showed efficiencies of 1.6%, but with limited light-harvesting again a significant performance limiting factor.[9] Here we introduce a new core-shell material as a pseudo-one dimensional ZnO photoanode produced from coating templates of high aspect ratio substructures, exhibiting initial efficiencies up to 2.4% under AM 1.5 illumination when incorporated in a DSSC.

Inert low density, high surface area silica aerogel films, featuring a large range of controllable thickness and porosity, are prepared as substructure templates. The aerogel templates are coated with ZnO via atomic layer deposition (ALD) to yield an electrically interconnected semiconductor core-shell nanoweb structure.[13,14] Because it is both a stepwise and conformal coating technique, ALD provides exceptional control over nanoscale device composition. The large number of materials accessible by ALD (including, but not limited to, TiO_2, ZnO, SnO_2, ZrO_2, and NiO) makes the technique widely applicable for the development of new photoelectrodes.[15] Herein we demonstrate the viability of ZnO versions of these structures as dye sensitized electrodes by characterizing their morphology, light harvesting efficiency, and photovoltaic performance.

Monolithic aerogel films were made with film thickness varying from 1–80 μm as determined from profilometry and SEM. The volume of sol dropcast onto the FTO substrate in general controls the film thickness. The porosity of aerogels is known to be controlled by the concentration of the sol and can be over 99% porous.[16,17] The aerogel films used in this study were not optimized for use in DSSCs; conditions were chosen, however, in order to make highly porous structures (>90%) in order to leave enough volume for growth of sufficiently thick ZnO layers without completely filling the aerogel pores. In addition, films approximately 25 μm thick were prepared for use as templates for the photoelectrodes described below.

The aerogel films as grown were extremely fragile; however, after they were coated with even a thin layer (>2 nm) of semiconductor, they were found to be very robust. Figure 1 shows SEM images of typical aerogel films coated with approximately

[*] Prof. J. T. Hupp, Dr. T. W. Hamann, A. B. F. Martinson, Prof. M. J. Pellin
Northwestern University
2145 Sheridan Rd, Evanston, IL 60208 (USA)
E-mail: j-hupp@northwestern.edu
A. B. F. Martinson, Dr. J. W. Elam, Prof. M. J. Pellin
Argonne National Laboratory
9700 S. Cass Avenue, Argonne, IL 60439 (USA)

[**] The SEM work was performed in the EPIC facility of NUANCE Center at Northwestern University. NUANCE Center is supported by NSF-NSEC, NSF-MRSEC, Keck Foundation, the State of Illinois, and Northwestern University. We gratefully acknowledge financial support from BP Solar, Argonne National Lab (fellowship for ABFM), and the U.S. Department of Energy, Basic Energy Sciences Program (Grant DE-FG02-87ER13808). We thank Tobin Marks for use of the solar cell analyzer. Supporting Information is available online from Wiley InterScience or from the authors.

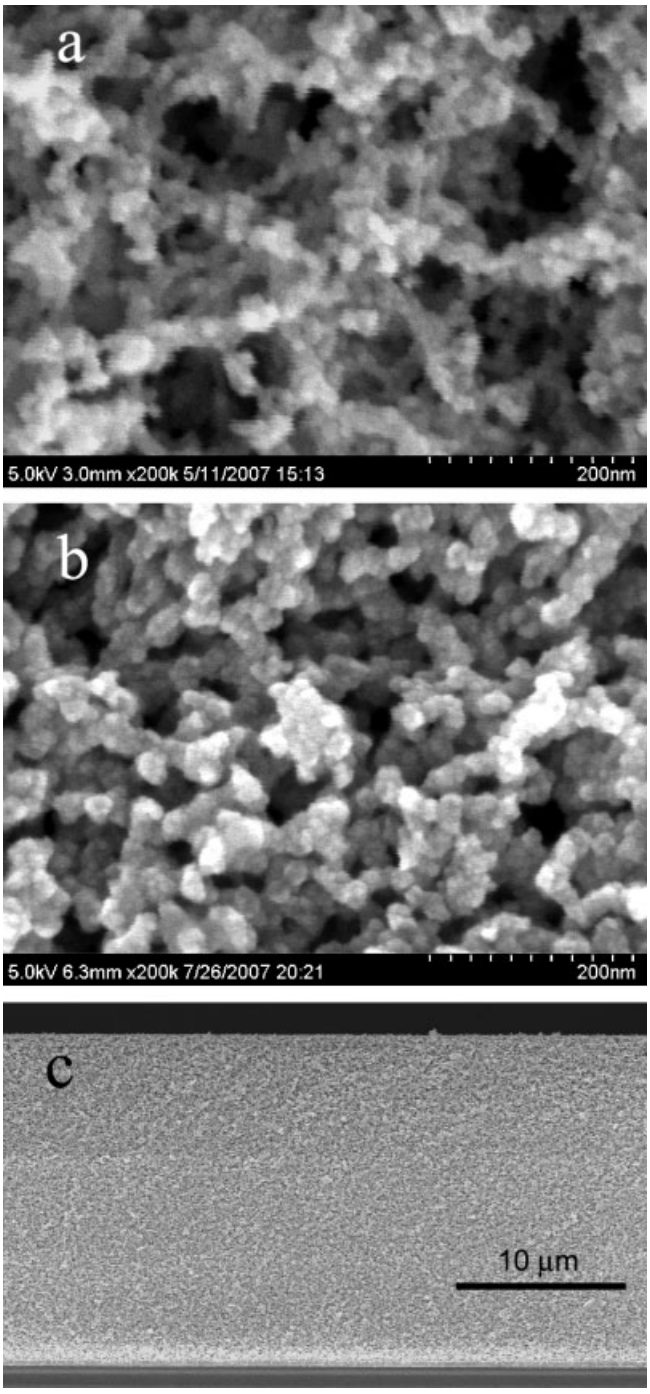

Figure 1. SEM images of aerogel frameworks coated with a) 4.4 and b) 8.4 nm ZnO and c) profile of typical film coated with 8.4 nm ZnO.

4.4 nm (21 cycles) and 8.4 nm (40 cycles) of ZnO. From the SEM images, the ZnO coatings appear conformal for each thickness of ZnO deposited, consistant with previous reports.[9,13] The aerogel films remain porous after coating with ZnO, and the porosity is observed to decrease as expected with additional growth of ZnO. In addition, the feature size of the coated aerogels closely matches twice the thickness of the deposited ZnO indicating that the original silica aerogel framework takes up a minimal amount of space as expected.

Aerogel films were coated with ZnO using 10, 20, 30, 40, or 50 ALD cycles. ZnO thicknesses were determined by ellipsometry measurements of flat silicon substrates that were coated concurrently in the ALD reactor. The measured thickness of ZnO deposited as a function of ALD cycles is linear with a rate of 0.21 nm/cycle, in good agreement with literature reports (Supporting Information Fig. 1).[18,19] Thus, the aerogel films were coated with approximately 2.1, 4.2, 6.3, 8.4, and 10.5 nm of ZnO. The aerogel films are transparent as deposited, then turn a translucent light yellow with thin coatings (<5 nm) of ZnO and finally become opaque-white due to scattering with thicker layers of ZnO.

In order to determine the dye loading of the ZnO coated aerogel films, dye molecules were desorbed from a nominally identical batch of electrodes. The absorbance from the dye desorbed from the aerogel electrode coated with 2.1 nm of ZnO in 3.0 mL 10 mM NaOH(aq) solution at 535 nm was 0.13. The N719 extinction coefficient at 535 nm is 1.474×10^4 L mol^{-1}, thus an absorbance of 0.13 indicates a concentration of 8.8×10^{-6} M or 1.6×10^{16} dye molecules. A first order approximation of the aerogel photoanode framework is a series of interconnected wires, i.e., cylinders, which suggests that the usable internal surface area should initially increase linearly with increasing thickness of ZnO, and subsequently decrease as the smaller pores of the aerogel close. This model is consistent with mass initially increasing with the square of the ALD film thickness, and subsequently becoming constant, as we have previously observed.[14,20] In fact, the absorbance decreased monotonically for the electrodes coated with ZnO layer thicknesses larger than 2.1 nm indicating that the usable surface area was decreasing, presumably due to pore filling (Table 1). Alternatively, since the porosity decreases with increasing ZnO thickness, poor diffusion of the dye throughout the aerogel membrane may be responsible for the decrease of dye loading with more ZnO. Poor diffusion is consistent with the observation of lighter coloration of the membrane on the back contact compared with the outside of the film. In any case, to the extent that they occur, both pore closing and inhibition of diffusion are likely to be detrimental in photoelectrode applications. For comparison, dye molecules desorbed from a 10 μm thick TiO_2 nanoparticle electrode in 3.0 mL 10 mM NaOH(aq) had and absorbance of 0.07 at 535 nm. Thus, the nanoparticle electrode had comparable dye loading to the aerogels films coated with 8.4 and 10.5 nm of ZnO.

Figure 2a shows the short-circuit current density, J_{sc}, as a function of ZnO thickness under AM 1.5 illumination. For the thinnest ZnO layers J_{sc} is low (0.26 mA cm^{-2} for 2.1 nm ZnO) and then rises with increasing thickness of ZnO. This trend of increasing J_{sc} with ZnO thickness is in contrast to the trend of decreasing dye loading. The increase in J_{sc} is therefore attributed to either better injection or charge collection efficiency. Another possible contribution is the internal scattering by the films featuring thicker layers of ZnO; scattering may increase light absorption due to the longer

ADVANCED MATERIALS

Table 1. Measured photovoltaic parameters.

ZnO [nm]	Absorbance [a] [a.u.]	Light intensity [W m^{-2}]	J_{sc} [mA cm^{-2}]	V_{oc} [V]	ff	η [%]
2.1	0.13	986	0.26	0.67	0.65	0.12
4.2	0.12	988	2.76	0.60	0.42	0.70
6.3	0.09	987	5.93	0.41	0.29	0.72
8.4	0.08	987	8.93	0.60	0.32	1.72
10.5	0.06	989	8.82	0.69	0.36	2.17
10.5 [b]	0.06	992	8.40	0.70	0.35	2.06
10.5 [c]	n/a	987	8.32	0.60	0.48	2.40

[a] Absorbance maximum at 532 nm ($\varepsilon = 1.47 \times 10^4$) for dye desorbed in 3.0 mL 10 mM NaOH from nominally identical batch of cells. [b] Backside illumination. [c] Cell with $[I_3^-] = 0.1$ M; for all other cells $[I_3^-] = 0.05$ M.

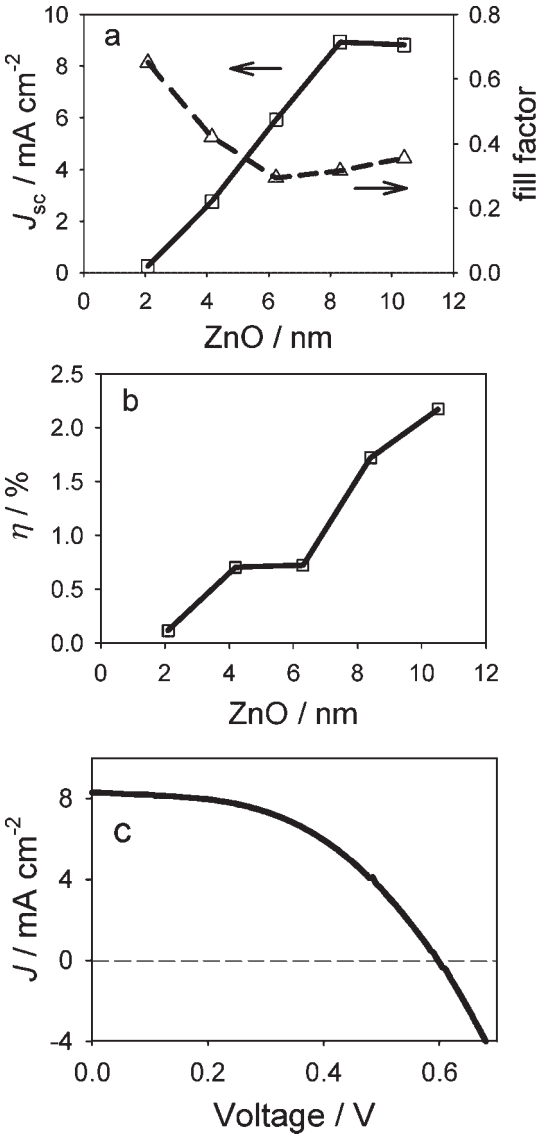

Figure 2. Plots of a) the short circuit current density (open squares), J_{sc}, and fill factor (filled triangles), b) efficiency, η, as a function of thickness of ZnO deposited on aerogel frameworks, and c) *J–V* curve for 2.4% efficient 10.5 nm ZnO electrode under AM 1.5 illumination (dashed line indicates zero current).

light path-length, thus enhancing J_{sc}. This thickness dependence is in excellent agreement with a report on ZnO nanotube DSSCs fabricated in anodic aluminum oxide, AAO, membranes.[9] Also shown in Figure 2a is a plot of the fill factor versus ZnO thickness. The fill factor is relatively high, 0.65, for the cell with 2.2 nm ZnO as expected for such low current densities, then quickly falls to 0.3–0.35 for the cells with thicker ZnO coatings. The low fill factors are a major limitation to the overall efficiencies of these cells. The open circuit potential (V_{oc}) of most cells varied between approximately 600 and 690 mV in an apparently random fashion. The cell with 6.6 nm of ZnO, however, had an anomalously low V_{oc} of 410 mV. Figure 2b shows the efficiency of the DSSC's measured under AM 1.5 illumination as a function of the deposited ZnO thickness. The efficiency (η) increases with increasing ZnO thickness mainly due to the increasing current densities. The maximum efficiency observed with this batch of electrodes was 2.2% corresponding to 10.5 nm of ZnO. Cells prepared with thicker layers of ZnO failed to load dye.

The relatively low fill factors and current densities, and hence efficiencies, are likely partially due to mass transport limitations. The deleterious effects due to mass transport manifest as a deviation from linearity in a plot of J_{sc} versus light intensity.[21] Figure 3a shows the measured J_{sc} under different light intensities for the photoanode coated with 10.5 nm ZnO. There are clearly mass transport problems at even modest illumination intensities that limit the efficiency of these aerogel cells at 1 sun. Figure 3a also shows that the backside illuminated J_{sc}, not corrected for expected 25% loss due to absorbance from the platinized counter electrode and by the electrolyte, is within 5% of J_{sc} illuminated through the photoelectrode. Since mass transport problems are partially overcome through backside illumination, the similarity of the uncorrected J_{sc}'s is consistent with mass transport current limitations. In addition, the large J_{sc} observed with backside illumination indicates that charge is likely collected throughout the 25 μm thick membrane.

Figure 3b shows the incident photon-to-current efficiency, IPCE, for the photoelectrode coated with 10.5 nm of ZnO. The measured photocurrents at a given wavelength are low and thus not limited by mass transfer. Integration of the photocurrent generated from incident light with wavelengths

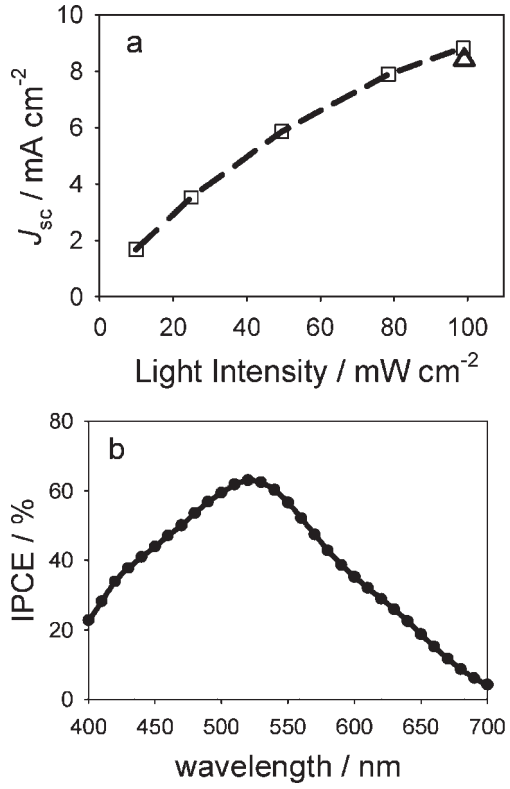

Figure 3. a) Short-circuit current density under different illumination intensities through the 10.5 nm ZnO photoelectrode (closed circles). Short-circuit current density under AM 1.5 illuminated through the counter electrode (open triangle). b) Incident photon-to-current efficiency (IPCE) of the 10.5 nm ZnO photoelectrode.

from 400–700 nm produces 11.5 mA cm^{-2}. This is a slight under-estimate of the expected J_{sc} under white light since it does not include contributions from wavelengths outside of the 400–700 nm range. Integration of the desorbed dyes absorbance with the AM 1.5 spectrum for the photoelectrode coated with 10.5 nm ZnO results in a maximum current density of 13 mA cm^{-2}. Thus, neglecting mass transport limitations, charge injection and collection throughout the 25 μm thick photoelectrode coated with 10.5 nm of ZnO is essentially quantitative.

Since the mass transport limiting current is proportional to triiodide concentration, film thickness and porosity, this limitation can likely be overcome through optimization of the aerogel film in combination with the electrolyte composition.[21] Other cells were prepared nominally identically as the series reported above. In an initial attempt to overcome mass transport limitations, the triiodide concentration was increased to 0.1 M in a cell employing an aerogel photoanode coated with 10.5 nm ZnO. The efficiency increased to 2.4% (Fig. 2c), with the higher efficiency due mainly to an improved fill factor. The improved cell performance with increased triiodide (electron acceptor) concentration is consistent with the expected faster electron transport. Further optimization of the many controllable parameters of the aerogel templated ZnO photoanode and electrolyte is expected to produce DSSCs with even greater efficiency.

In summary, a new pseudo one-dimensional architecture for DSSC photoanodes was prepared using templates of low-density, high surface area, mesoporous aerogel thin films. ZnO was conformally deposited with a controlled variable thickness on the aerogel templates by ALD. The electrodes incorporated into DSSCs displayed good light harvesting efficiency and excellent power efficiencies compared with other ZnO based DSSCs.[8,9,22–24] A major limitation to the overall efficiency was found to be mass transport. The excellent initial performance reported herein, the ease of fabrication, and the flexibility of design make ALD coated aerogel templated photoanodes a promising candidate to move beyond nanoparticle electrodes in DSSCs.

Experimental

All chemicals, unless noted otherwise, were purchased from Aldrich and used as received.

Aerogel films were prepared as follows. A silica solution was prepared by diluting a prehydrolyzed ethyl polysilicate solution (Silbond corp.) to 50% by volume with ethanol. One volume equivalent of a catalyst solution (50 mL H_2O, 40 mL ethanol, 1.6 mL 30% NH_4OH) was slowly added while stirring to the silica solution to form the sol. Prior to the gel point, typically 10 min, the sol was dropcast onto fluorine-doped tin oxide, FTO, substrates inside a controlled atmosphere chamber saturated with 1:1 ethanol:water vapor. The gel point was approximately 20 min. Following gelation, substrates were immersed in catalyst solution and allowed to react an additional 12 hours. The resulting alcogel films were exchanged with ethanol three times to remove residual water and dried with supercritical CO_2. The aerogel active areas were 0.25 cm^2, defined by scraping with a razor blade.

ALD was performed with a Savannah 100 (Cambridge Nanotech Inc.) using diethyl zinc, DEZ, and water as precursors. ZnO was grown at 150 °C using reactant exposure times of 20 and 10 s and partial pressures of 2 and 10 Torr for DEZ and H_2O, respectively, with 30 s nitrogen purge times between exposures. The ZnO coated films were heated to 450 °C in air for 20 minutes to increase crystallinity.

After heating the substrates were cooled to 100 °C and immediately introduced to 0.5 mM $(Bu_4N)_2[Ru(4,4'\text{-}(COOH)\text{-}2,2'\text{-bipyridine})_2(NCS)_2]$ (“N719”, Dyesol, B2 dye) in ethanol for 30 min, rinsed with ethanol, and dried with nitrogen. A Surlyn frame was sandwiched between the photoanode and a platinized FTO electrode. Light pressure was applied at 80 °C to seal the cell. A solution of 0.5 M LiI, 0.05 mM I_2, and 0.5 M *t*-butylpyridine in 3-methoxypropionitrile was introduced into the ZnO cells via vacuum backfilling through a hole in the platinized FTO electrode. Additional Surlyn and a microscope cover slip sealed the electrolyte into the cell.

AM 1.5 efficiencies were measured on a Class A solar cell analyzer from Spectra-Nova Technologies with a power of ≈985 W m^{-2} (Table 1). Absorbance was measured using a Varian Cary 5000 UV-Vis spectrometer. Film thicknesses were measured on a Tencor P10 profilometer. Scanning electron microscopy (SEM) images were collected on a Hitachi S-4800-II cFEG SEM.

Received: November 9, 2007
Revised: December 18, 2007

ADVANCED MATERIALS

[1] M. Grätzel, *Inorg. Chem.* **2005**, *44*, 6841.
[2] M. K. Nazeeruddin, F. DeAngelis, S. Fantacci, A. Selloni, G. Viscardi, P. Liska, S. Ito, B. Takeru, M. Grätzel, *J. Am. Chem. Soc.* **2005**, *127*, 16835.
[3] J. M. Kroon, N. J. Bakker, H. J. P. Smit, P. Liska, K. R. Thampi, P. Wang, S. M. Zakeeruddin, M. Grätzel, A. Hinsch, S. Hore, U. Wurfel, R. Sastrawan, J. R. Durrant, E. Palomares, H. Pettersson, T. Gruszecki, J. Walter, K. Skupien, G. E. Tulloch, *Prog. Photovoltaics* **2007**, *15*, 1.
[4] L. M. Peter, *J. Phys. Chem. C* **2007**, *111*, 6601.
[5] B. A. Gregg, *Coord. Chem. Rev.* **2004**, *248*, 1215.
[6] B. A. Gregg, F. Pichot, S. Ferrere, C. L. Fields, *J. Phys. Chem. B* **2001**, *105*, 1422.
[7] S. Cazzanti, S. Caramori, R. Argazzi, C. M. Elliott, C. A. Bignozzi, *J. Am. Chem. Soc.* **2006**, *128*, 9996.
[8] M. Law, L. E. Greene, J. C. Johnson, R. Saykally, P. D. Yang, *Nat. Mater.* **2005**, *4*, 455.
[9] A. B. F. Martinson, J. W. Elam, J. T. Hupp, M. J. Pellin, *Nano Lett.* **2007**, *7*, 2183.
[10] M. Paulose, K. Shankar, O. K. Varghese, G. K. Mor, B. Hardin, C. A. Grimes, *Nanotechnology* **2006**, *17*, 1446.
[11] E. Galoppini, J. Rochford, H. Chen, G. Saraf, Y. Lu, A. Hagfeldt, G. Boschloo, *J. Phys. Chem. B* **2006**, *110*, 16159.
[12] A. B. F. Martinson, J. E. McGarrah, M. O. K. Parpia, J. T. Hupp, *Phys. Chem. Chem. Phys.* **2006**, *8*, 4655.
[13] S. O. Kucheyev, J. Biener, Y. M. Wang, T. F. Baumann, K. J. Wu, T. van Buuren, A. V. Hamza, J. H. Satcher, J. W. Elam, M. J. Pellin, *Appl. Phys. Lett.* **2005**, *86*.
[14] J. W. Elam, G. Xiong, C. Y. Han, H. H. Wang, J. P. Birrell, U. Welp, J. N. Hryn, M. J. Pellin, T. F. Baumann, J. F. Poco, J. H. Satcher, *J. Nanomater.* **2006**, *2006*, 1.
[15] M. Ritala, M. Leskela, in *Handbook of Thin Film Materials*, Vol. 1(Ed: H. S. Nalwa), Academic, San Diego, CA **2001**, p. 103.
[16] Y. K. Akimov, *Instrum. Exp. Tech.* **2003**, *46*, 287.
[17] J. Fricke, T. Tillotson, *Thin Solid Films* **1997**, *297*, 212.
[18] E. B. Yousfi, J. Fouache, D. Lincot, *Appl. Surf. Sci.* **2000**, *153*, 223.
[19] J. W. Elam, Z. A. Sechrist, S. M. George, *Thin Solid Films* **2002**, *414*, 43.
[20] J. W. Elam, J. A. Libera, M. J. Pellin, A. V. Zinovev, J. P. Greene, J. A. Nolen, *Appl. Phys. Lett.* **2006**, *89*.
[21] N. Papageorgiou, M. Grätzel, P. P. Infelta, *Sol. Energy Mater. Sol. Cells* **1996**, *44*, 405.
[22] T. P. Chou, Q. Zhang, G. E. Fryxell, G. Z. Cao, *Adv. Mater.* **2007**, *19*, 2588.
[23] E. Hosono, S. Fujihara, I. Honna, H. S. Zhou, *Adv. Mater.* **2005**, *17*, 2091.
[24] K. Keis, E. Magnusson, H. Lindstrom, S. E. Lindquist, A. Hagfeldt, *Sol. Energy Mater. Sol. Cells* **2002**, *73*, 51.